JOURNAL OF MATERIALS SCIENCE 27 (1992) 6223–6228

# Mössbauer spectroscopic studies of glass ceramics with hexagonal barium and strontium ferrites

U. C. JOHRI, R. M. SINGRU *
*Department of Physics, Indian Institute of Technology, Kanpur-208 016, India*
D. BAHADUR ‡
*Materials Science Center, Indian Institute of Technology, Bombay-400 076, India*

Mössbauer spectroscopic studies have been performed on glass ceramics in which barium and strontium hexaferrites have been crystallized as a major magnetic phase. The crystallization process of the different magnetic phases has been studied by suitable heat treatments of the initial glass compositions $35BaO–40B_2O_3–25Fe_2O_3$, $35SrO–40B_2O_3–25Fe_2O_3$ and $47SrO–28B_2O_3–25Fe_2O_3$. The nucleation and growth times have been varied and Mössbauer spectra of differently heat-treated samples analysed to determine the optimum composition and heat treatment required for the good growth of the hexagonal ferrites BaM and SrM.

## 1. Introduction

In recent years barium ferrite particulate media have invoked considerable research interest because of their interesting digital and analogue applications such as the possibility of superior recording performance at relatively low cost [1]. Barium ferrite particulate media have been utilized as promising high-density recording media in fields ranging from audio and video recorders to flexible disk memories.

At this Institute, Ram *et al.* [2] have developed glass ceramics in which barium and strontium hexaferrites have been crystallized in the borate glass systems $MO–B_2O_3–Fe_2O_3$ (M = Ba or Sr). The optimum conditions for crystallization of the hexaferrite phase have been examined by them by varying the time period for nucleation and growth. They concluded that the hexaferrite is the major magnetic crystalline phase in most of the samples and the microstructure, coercivity and other magnetic properties are strongly dependent on the heat-treatment schedule. We therefore thought it interesting to study the magnetic phases in the borate glasses $MO–B_2O_3–Fe_2O_3$ (M = Ba or Sr) by Mössbauer spectroscopy. It is known that Mössbauer spectroscopy, being more sensitive than X-ray diffraction and magnetic measurements in the identification of phases, can, in principle, delineate the crystallization of phases and their comparative volume fractions. With this aim in mind the samples of $MO–B_2O_3–Fe_2O_3$ were subjected to different schedules of heat treatments and the Mössbauer spectra of these heat-treated samples were investigated. The present results have also been analysed to indicate the optimum composition and heat treatment that can lead to a good growth of the hexagonal ferrites BaM and SrM.

## 2. Experimental procedure

The glass compositions prepared for the present work were (i) $35BaO–40B_2O_3–25Fe_2O_3$, (ii) $35SrO–40B_2O_3–25Fe_2O_3$ and (iii) $47SrO–28B_2O_3–25Fe_2O_3$ and these were labelled as B10, S10 and S20, respectively. The glasses were prepared by melting and casting the required mixture of oxides (reagent grade chemicals) in an alumina crucible between 1400 K and 1750 K in an electrically heated furnace. The glass transition, $T_g$, and crystallization, $T_c$, temperatures were estimated from the differential thermal analysis (DTA) plots obtained on an MOM Hungary derivatograph. The samples were then heat treated in two successive steps at various combinations of nucleation and growth temperatures to obtain ceramized glasses. The schedule of heat treatment given to these samples is described in Table I where the temperatures and time periods of the nucleation and crystallization stages are given. X-ray powder diffraction patterns for glass ceramic samples were recorded in a Rich and Seifert ISO-Debyeflex 2002 diffractometer with $CrK_\alpha$ target. The as-prepared as well as the heat-treated glasses were powdered and suitable absorbers for Mössbauer spectroscopy were prepared for measurements which were performed at room temperatures (RT) with a constant acceleration (linear mode) Mössbauer spectrometer coupled to a multichannel analyser. The

* *Current address*: Institut fur Nukleare Feskorperphysik, Fakultät CRT, UniBWM, Werner-Heisenberg-Weg 39, D-8014 Neubiberg, Germany.
‡ On leave from Advanced Center for Materials Science, Indian Institute of Technology, Kanpur-208 016, India.

0022–2461  

TABLE I Sample labels and details of heat treatment given to different glass compositions (heat treatment is described in terms of temperature (K)/time period (h)) with X-ray and magnetization data

| Composition | Heat treatment (temperature (K)/time period (h)) | Sample label | Crystalline phase identified from X-ray analysis[a] (S, strong, W, weak) | $M^b$(e.m.u. $g^{-1}$) at $H = 7.958 \times 10^5$ A $m^{-1}$ [a] | $H_c^c$(A $m^{-1}$) | $T_\theta^d$(K)[a] |
|---|---|---|---|---|---|---|
| $35BaO-40B_2O_3-25Fe_2O_3$ | | B10 | – | – | – | – |
| | 850/2 + 895/20 | B1 | – | – | – | – |
| | 850/2 + 1015/20 | B2 | – | – | – | – |
| | 850/2 + 1065/2 | B3 | $BaFe_{12}O_{19}$ and $\alpha$-$Fe_2O_3$ (W) | 14.0 | $3.98 \times 10^4$ | 635, 725 |
| | 850/2 + 1065/20 | B4 | $BaFe_{12}O_{19}$ (S), $\alpha$-$Fe_2O_3$ (W) | – | – | – |
| | 975/2 + 1015/2 | B5 | Barium borate (W), $\alpha$-$Fe_2O_3$ (W) and $BaFe_{12}O_{19}$ (S) | 13.5 | $2.5 \times 10^4$ | 590, 750 |
| | 1035/2 + 1065/2 | B6 | $BaFe_{12}O_{19}$ (single phase) | 11.5 | $8.35 \times 10^4$ | 720 |
| | | S10 | – | – | – | – |
| $35SrO-40B_2O_3-25Fe_2O_3$ | 885/5 + 1035/10 | S11 | $SrFe_{12}O_{19}$ (S) | 7.3 | $3.06 \times 10^4$ | 750, 850 |
| | 965/2 + 1120/10 | S12 | $SrFe_{12}O_{19}$ (S), $\alpha$-$Fe_2O_3$ (W) | 7.2 | $1.87 \times 10^4$ | 750, 850 |
| | | S20 | – | – | – | – |
| $47SrO-28B_2O_3-25Fe_2O_3$ | 1100/2 + 1135/25 | S21 | $SrFe_{12}O_{19}$ (S), $\alpha$-$Fe_2O_3$ (W) | 4.5 | $3.42 \times 10^5$ | 730, 830 |

[a] Refs 2 and 17.
[b] $M$, Magnetization.
[c] $H_c$, Coercive field.
[d] $T_\theta$, Curie temperature.

source used was radioactive $^{57}Co$ in Rh matrix obtained from New England Nuclear Inc., USA. The spectrometer was calibrated by using the enriched $^{57}Fe$ powder. A least-squares curve-fitting computer program was used to determine the Mössbauer parameters and the standard errors in these parameters were calculated by the usual methods.

## 3. Results and discussion

The Mössbauer spectra for the as-prepared borate glass samples B10, S10 and S20 measured at RT were observed to be similar and they all showed three lines that could be decomposed into two doublets. Such an analysis of a representative sample S20 is shown in Fig. 1 and it yielded the following set of Mössbauer parameters for the two doublets: (i) Isomer shift ($I_S$) = $+0.445 \pm 0.005$ mm $s^{-1}$ (with respect to $\alpha$-Fe) quadrupole splitting, $\Delta E = 1.040 \pm 0.010$ mm $s^{-1}$ and the line-width (FWHM), $\Gamma = 0.58 \pm 0.01$ mm $s^{-1}$. This spectrum can be assigned to $Fe^{3+}$ in six coordination with $O^{2-}$ ions [3, 4] and (ii) $I_S = +0.977 \pm 0.005$ mm $s^{-1}$, $\Delta E = 2.6 \pm 0.01$ mm $s^{-1}$ and $\Gamma = 0.58 \pm 0.01$ mm $s^{-1}$. This spectrum is attributed to $Fe^{2+}$ in glassy medium [5]. The large values of the line-widths ($\Gamma$) observed by us are characteristic of borate (and other) glasses.

The Mössbauer spectra of the samples B1, B2, B3, B4, B5 and B6 (Table I) are shown in Figs 2 and 3. Although these spectra appear complex, we tried to look for the presence of the magnetic phases $BaFe_{12}O_{19}$ and $\alpha$-$Fe_2O_3$ because these phases were identified by the X-ray analysis [2]. It has been observed that the Mössbauer spectrum of $BaFe_{12}O_{19}$ consists of five sextets arising out of five different magnetic sublattices [6, 7]. The sublattice magnetization of $BaFe_{12}O_{19}$ has been studied by Van Loef and Franssen [8] and by Kreber *et al.* [9] while the

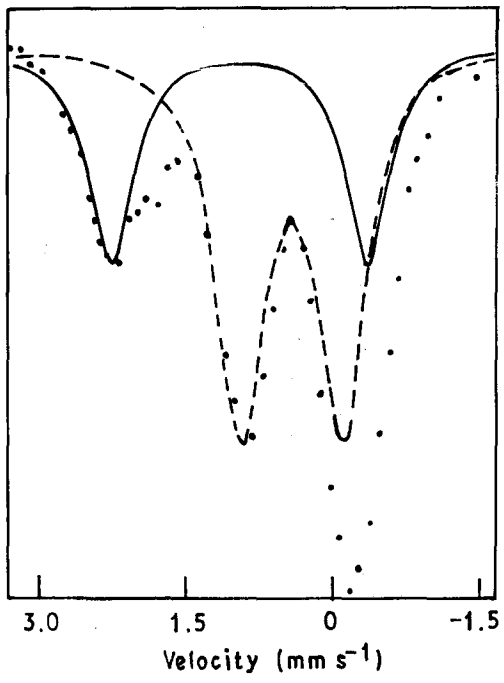


*Figure 1* Mössbauer spectrum of sample S20 at 293 K.

fundamental properties of hexagonal ferrites with magnetoplumbite structure have been reviewed elsewhere [10, 11]. The Mössbauer parameters of the five sextets assigned to $BaFe_{12}O_{19}$ from the analysis of our data for the heat-treated samples (B1 to B6) are given in Table II. The assignments of the sublattice (labels a, b, c, d and e) have been made on the basis of the internal magnetic field ($H_{int}$) values reported by Van Loef and Franssen [8] and Kreber *et al.* [9]. It may be pointed out that the value of $H_{int}$ (for each sublattice) obtained for the B1 sample appears much lower than the corresponding $H_{int}$ values for other (B2 to B6) samples. We ascribe this behaviour to the effect of superparamagnetism arising out of the small particle size of $BaFe_{12}O_{19}$ in the sample B1 since its second-stage heating was done at 895 K as compared with above 1010 K for other samples (see Table I). In view of this behaviour, the sublattices were assigned using the $H_{int}$ values of the samples B2 to B6. The sublattices in the sample B1 were assigned by examining the values of $I_S$ and $\Delta E$ and by comparing them with the values for the other samples B2 to B6.

The Mössbauer parameters of the $\alpha$-$Fe_2O_3$ phase present in varying degrees in the samples B1–B6 are also shown in Table II. It is also observed that the volume fraction of $\alpha$-$Fe_2O_3$, as deduced from Mössbauer spectra, is smaller in samples B3, B5 and B6. The samples B3, B5 and B6 have been studied previously by Ram *et al.* [2] and their results for the values of magnetization $M$ and coercive field $H_c$, Curie temperature $T_\theta$ as well as the crystalline phases identified by them from X-ray analysis are shown in Table I.

The present studies have enabled us to identify different magnetic phases and optimum temperatures and time periods for the maximum volume fraction of BaM in the present glass system. The $\alpha$-$Fe_2O_3$ phase appears to be present in all the samples (B1–B6) although in varying proportion. The X-ray diffraction studies [2], however, have revealed the presence of the BaM phase only (but no $\alpha$-$Fe_2O_3$) in B6. The Mössbauer spectra, by virtue of their higher sensitivity, are able to show a minute fraction of $\alpha$-$Fe_2O_3$ phase even in sample B6, apparently not detected by X-rays.

According to the results of our Mössbauer measurements (Figs 2 and 3) the maximum volume fraction of BaM is present in sample B4. It is indicated, on the basis of Mössbauer measurements, that the optimum nucleation temperature is 850 K and optimum crystallization temperature is 1065 K with time periods of 2 h and 20 h, respectively (Table II). The presence of $\alpha$-$Fe_2O_3$ is indicated in B1 by the intense lines characteristic of this compound. While going from sample B1 to sample B2, the nucleation temperature (850 K) and time period (2 h) (Table I) remain the same but the crystallization temperature is increased from 895 to 1015 K. This has led to a reduction in the volume fraction of $\alpha$-$Fe_2O_3$ (Fig. 2). We also observed that the volume fraction of different phases is also affected by the time period of heat treatment given to the samples. Going from sample B3 to B4 the nucleation temperature and the time period as well as the crystallization temperature remain the same but the time period for

TABLE II Mössbauer parameters of samples B1, B2, B3, B4, B5 and B6 at 293 K

| Sample label | Mössbauer parameters of different phases present in samples | | | | | | | | | | | | | | | | | | | |
|---|---|---|---|---|---|---|---|---|---|---|---|---|---|---|---|---|---|---|---|---|
| | Phase $BaFe_{12}O_{19}$ (five different magnetic sites in $BaFe_{12}O_{19}$) | | | | | | | | | | | | | | | | Phase $\alpha$-$Fe_2O_3$ | | | |
| | I(a) | | | II(c) | | | III(d) | | | IV(e) | | | V(b) | | | | | | | |
| | $I_S$[a] | $\Delta E$[b] | $H_{int}$[c] ($\times 10^7$) | $I_S$ | $\Delta E$ | $H_{int}$ ($\times 10^7$) | $I_S$ | $\Delta E$ | $H_{int}$ ($\times 10^7$) | $I_S$ | $\Delta E$ | $H_{int}$ ($\times 10^7$) | $I_S$ | $\Delta E$ | $H_{int}$ ($\times 10^7$) | $I_S$ | $\Delta E$ | $H_{int}$ ($\times 10^7$) |
| B1 | 0.32 | 0.10 | 3.10 | 0.24 | 0.05 | 3.34 | 0.36 | 0.12 | 3.58 | 0.15 | 1.40 | 3.33 | 0.38 | 0.06 | 3.34 | 0.36 | −0.11 | 4.07 |
| B2 | 0.39 | 0.19 | 3.25 | 0.22 | 0.09 | 3.78 | 0.37 | 0.09 | 4.09 | 0.13 | 1.40 | 3.34 | 0.36 | 0.09 | 3.70 | 0.36 | −0.11 | 4.07 |
| B3 | 0.35 | 0.13 | 3.33 | 0.24 | 0.09 | 3.82 | 0.34 | 0.10 | 4.06 | 0.12 | 1.37 | 3.46 | 0.40 | 0.03 | 3.66 | 0.36 | −0.11 | 4.07 |
| B4 | 0.36 | 0.12 | 3.34 | 0.22 | 0.09 | 3.86 | 0.34 | 0.10 | 4.06 | 0.10 | 1.42 | 3.34 | 0.39 | 0.05 | 3.62 | – | – | – |
| B5 | 0.37 | 0.13 | 3.34 | 0.23 | 0.06 | 3.82 | 0.38 | 0.12 | 4.07 | 0.11 | 1.48 | 3.36 | 0.36 | 0.08 | 3.66 | 0.36 | −0.11 | 4.10 |
| B6 | 0.36 | 0.13 | 3.34 | 0.22 | 0.08 | 3.82 | 0.36 | 0.12 | 4.06 | 0.11 | 1.46 | 3.34 | 0.36 | 0.06 | 3.70 | 0.36 | −0.11 | 4.07 |

[a] $I_S$, Isomer shift value in mm s$^{-1}$ with respect to $\alpha$-Fe; typical error is $\pm$ 0.02 mm s$^{-1}$.
[b] $\Delta E$, Quadrupole splitting in mm s$^{-1}$; typical error is $\pm$ 0.02 mm s$^{-1}$.
[c] $H_{int}$, Internal magnetic field at $^{57}$Fe nucleus in A m$^{-1}$; typical error is $\pm 4.77 \times 10^5$ A m$^{-1}$.

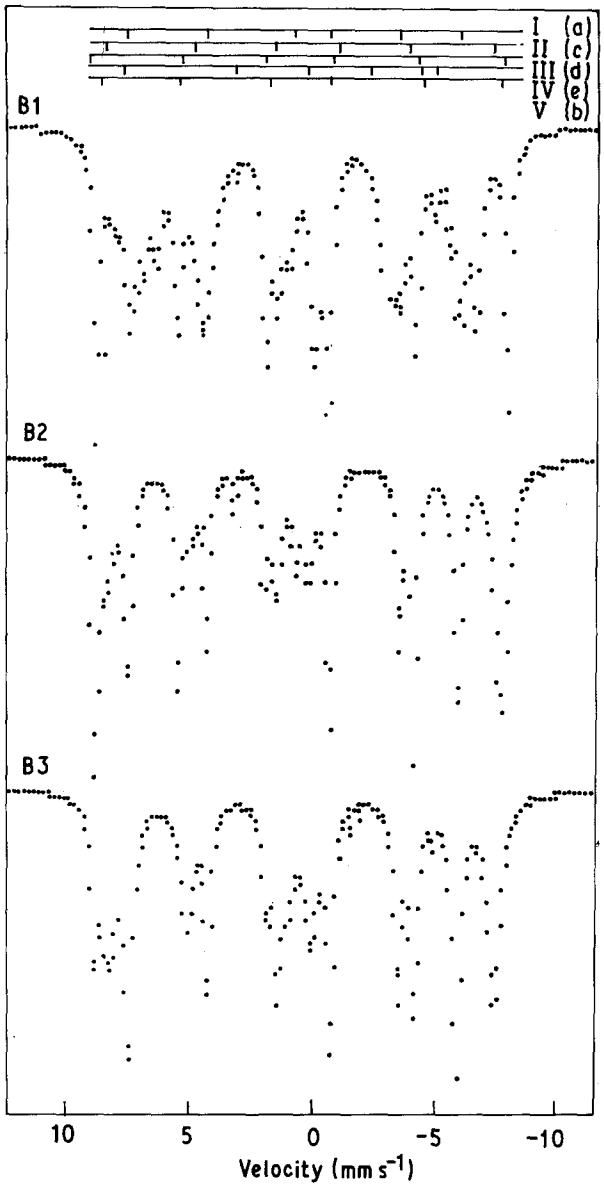


*Figure 2* Mössbauer spectra of samples B1, B2, and B3 at 293 K.

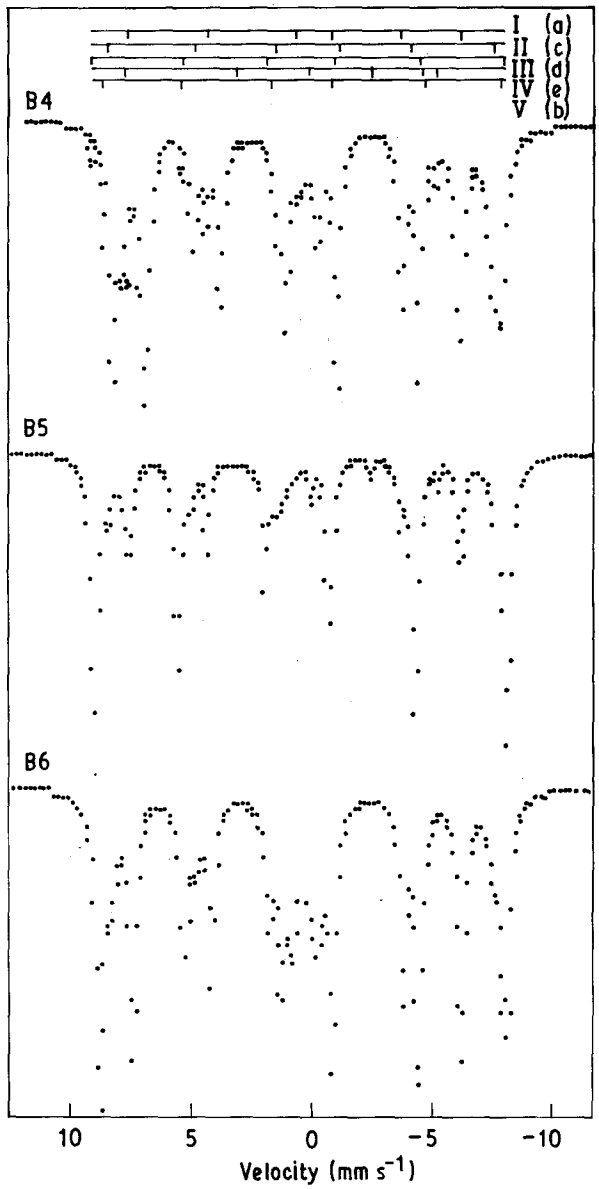


*Figure 3* Mössbauer spectra of samples B4, B5, and B6 at 293 K.

the crystallization stage is increased from 2 h to 20 h. This has resulted in the reduction of the volume fraction of the $\alpha$-$Fe_2O_3$ phase. It is possible that the increase in the crystallization time period helped $Fe_2O_3$ and barium borate to react and to give rise to BaM. Similar results were reported by Beretka and Ridge [12] in the case of the synthesis of BaM from a mixture of barium carbonate and iron oxide. These authors found that $BaFe_2O_4$ is formed as an intermediate product which further reacts with $Fe_2O_3$ to give BaM. In the case of our present composition it is likely that $BaB_2O_9$ is the main intermediate product because the temperature of heat treatment is much lower than that used for the ceramic method [12].

We shall now discuss the results of our studies of the systems $35SrO$–$40B_2O_3$–$25Fe_2O_3$ and $47SrO$–$28B_2O_3$–$25Fe_2O_3$ through samples S11, S12 and S21 (Table I). It is seen from Fig. 4 that the Mössbauer spectra of all these three samples (S11, S12 and S21) show a non-flat baseline which is an indication of the effect of spin-fluctuation arising out of superparamagnetism [13]. In the case of sample S11, the Mössbauer lines corresponding to $\alpha$-$Fe_2O_3$ are seen distinctly with the relevant Mössbauer parameters as $I_S = 0.36 \pm 0.01\ mm\,s^{-1}$, $\Delta E = -0.12\ mm\,s^{-1}$ and $H_{int} = 4.098 \times 10^7 \pm 53.98 \times 10^5\ A\,m^{-1}$. In addition to the lines arising out of $\alpha$-$Fe_2O_3$, the spectrum of sample S11 shows the presence of other lines which are assigned to the five magnetic sublattices of $SrFe_{12}O_{19}$ (SrM) as suggested by Kreber *et al.* [9] and Belov *et al.* [14]. Following Kreber *et al.* [9] we observe that the lines due to the sublattice V(b) and III(d) appear too close to be resolved while the other lines due to the sublattices I(a), II(c) and IV(e) appear resolved (Fig. 4). The Mössbauer parameters for the sublattice of $SrFe_{12}O_{19}$ as analysed by us from our spectra are shown in Table III where these results are also compared with the Mössbauer parameters reported by Belov *et al.* [14] for $SrFe_{12}O_{19}$. It is seen that there is good agreement between our results and those obtained by Belov *et al.* [14]. We, however, observe from our spectra that the intensity of the spectral lines due to V(b) and III(d) sublattices is lower than those due to the I(a) and II(c) sublattices. We ascribe this behaviour

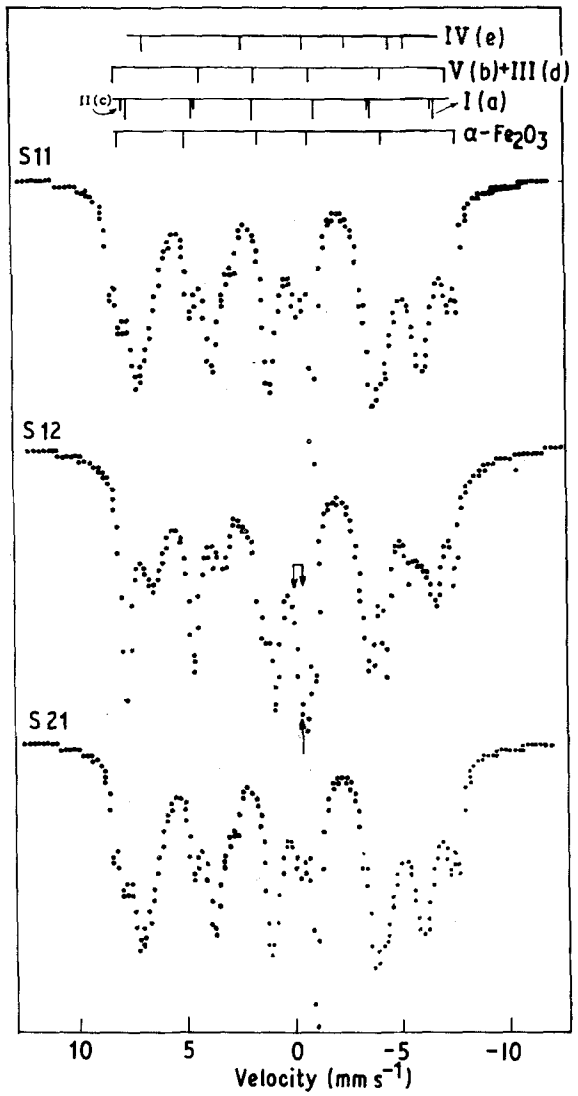


*Figure 4* Mössbauer spectra of samples S11, S12, and S21 at 293 K.

to the presence of $\alpha$-$Fe_2O_3$ along with SrM in our samples, which make the computer analysis of the spectra difficult. We further point out that the X-ray analysis (see Table I) does not reveal the presence of $\alpha$-$Fe_2O_3$ in sample S11. Once again this type of behaviour shows that the two techniques, X-ray diffraction and Mössbauer spectroscopy, differ in their sensitivities.

The Mössbauer spectrum for sample S12 shows the presence of spectral lines from $\alpha$-$Fe_2O_3$ and SrM (Fig. 4) although the amount of $\alpha$-$Fe_2O_3$ in sample S12 appears to be lower than that in sample S11. It is further observed that the intensity of the low-velocity lines is higher in the Mössbauer spectrum of sample S12 and this suggests the presence of phases other than $\alpha$-$Fe_2O_3$ and SrM. These additional phases could be $Sr_3Fe_2O_{6.9}$ and $SrFe^{IV}O_3$–$SrFe^{III}O_{2.5}$. However, the Mössbauer spectrum of $SrFe^{IV}O_3$–$SrFe^{III}O_{2.5}$ is known to give a single line [15] at a velocity indicated by a dotted arrow in Fig. 4. It is seen that at this velocity the line due to $SrFe^{IV}O_3$–$SrFe^{III}O_{2.5}$ is totally masked by the line due to $\alpha$-$Fe_2O_3$ and SrM. It is therefore difficult to confirm the presence of $SrFe^{IV}O_3$–$SrFe^{III}O_{2.5}$ in our spectra. It has been reported that $Sr_3Fe_2O_{6.9}$ gives rise to three lines in the Mössbauer spectrum with a singlet due to

TABLE III Mössbauer parameters of samples S11, S12 and S21 at 293 K

| Sample label | Mössbauer parameters of different phases present in samples[a] | | | | | | | | | | | | | | | | | |
|---|---|---|---|---|---|---|---|---|---|---|---|---|---|---|---|---|---|---|
| | Phase $SrFe_{12}O_{19}$ (five different magnetic sites in $SrFe_{12}O_{19}$) | | | | | | | | | | | | | | Phase $\alpha$-$Fe_2O_3$ | | | |
| | I(a) | | | II(c) | | | III(d) | | | IV(e) | | | V(b) | | | | | |
| | $I_S$ | $\Delta E$ | $H_{int}$ ($\times 10^7$) | $I_S$ | $\Delta E$ | $H_{int}$ ($\times 10^7$) | $I_S$ | $\Delta E$ | $H_{int}$ ($\times 10^7$) | $I_S$ | $\Delta E$ | $H_{int}$ ($\times 10^7$) | $I_S$ | $\Delta E$ | $H_{int}$ ($\times 10^7$) | $I_S$ | $\Delta E$ | $H_{int}$ ($\times 10^7$) |
| S11[b] | 0.43 | 0.22 | 3.34 | 0.36 | 0.04 | 3.94 | 0.42 | 0.18 | 4.06 | 0.22 | 1.08 | 3.26 | 0.42 | 0.18 | 4.06 | 0.36 | − 0.11 | 4.07 |
| S12[b] | 0.46 | 0.26 | 3.26 | 0.32 | 0.06 | 3.86 | 0.40 | 0.15 | 4.07 | 0.23 | 1.10 | 3.26 | 0.40 | 0.15 | 4.07 | 0.36 | − 0.11 | 4.07 |
| S21 | 0.46 | 0.24 | 3.30 | 0.35 | 0.06 | 3.86 | 0.42 | 0.15 | 4.10 | 0.24 | 1.08 | 3.26 | 0.42 | 0.15 | 4.10 | 0.36 | − 0.11 | 4.07 |

[a] For definitions of $I_S$, $\Delta E$ and $H_{int}$, see Table II.
[b] In sample S12 and S21 $Sr_3Fe_2O_{6.2}$ is also present. The Mössbauer parameters for S12: $I_S = -0.32$; $I_S = 0.32$ and $\Delta E = 0.40$. The Mössbauer parameters for S21: $I_S = -0.34$; $I_S = 0.33$ and $\Delta E = 0.42$.

$Fe^{IV}$ with $I_S = -0.32\,mm\,s^{-1}$ and a doublet due to $Fe^{3+}$ with $I_S = 0.32\,mm\,s^{-1}$ and $\Delta E = 0.40\,mm\,s^{-1}$. We have indicated the expected peak position of these three lines due to $Sr_3Fe_2O_{6.9}$ in our spectrum (Fig. 4) by solid arrows. We feel, therefore, that there is evidence for the presence of $Sr_3Fe_2O_{6.9}$ phase in the sample S12 as revealed by our Mössbauer spectrum. In Table III we have given the Mössbauer parameters of $Sr_3Fe_2O_{6.9}$ as analysed from our spectra.

The Mössbauer spectrum of sample S21 also shows the presence of $\alpha$-$Fe_2O_3$, SrM and $Sr_3Fe_2O_{6.9}$ (Fig. 4). The Mössbauer parameters obtained for sample S21 are given in Table III, where it is observed that the experimental errors are relatively larger for the sample S21. This effect is due to the fact that different lines in the Mössbauer spectrum for sample S21 are poorly resolved. It is worth mentioning that the composition of sample S21 ($47SrO–28B_2O_3–25Fe_2O_3$) is different from that of the samples S11 and S12 ($35SrO–40B_2O_3–25Fe_2O_3$).

A comparison of the results for the three samples S11, S12 and S21 is in order here. All these three samples show the presence of $\alpha$-$Fe_2O_3$ and SrM while the samples S12 and S21 which have been given higher temperature heat treatment indicate the presence of the additional phase $Sr_3Fe_2O_{6.9}$. Our results indicate that heat treatment similar to one used by us for the sample S11 involving lower temperatures for nucleation (at $\sim 885$ K for 5 h) and crystallization (at $\sim 1035$ K for 10 h) is preferable.

In summary, we have studied the Mössbauer spectra of glass ceramics in which magnetic phases of barium and strontium hexaferrites have been crystallized after heat treatment. These studies have provided useful information about the crystallization process involving these magnetic phases.

## Acknowledgements

The authors are grateful to Dr D. Chakravorty for valuable discussions. This work was partly supported by CSIR, Government of India.

## References

1. T. FUJIWARA, *IEEE Trans. Mag.* **MAG-21** (1985) 1480 and references cited therein.
2. S. RAM, D. BAHADUR and D. CHAKRAVORTY, Proceedings of the XIV International Congress on Glass, New Delhi, India, Vol. 1 (Indian Ceramic Society, 1986) p. 336.
3. M. J. TRICKER, J. M. THOMAS, M. H. OMAR, A. OSMAN and A. BISHAY, *J. Mater. Sci.* **9** (1974) 1115.
4. E. BURZO and DOIRA UNGUR, *Mater. Res. Bull.* **17** (1982) 935.
5. T. NISHIDA, T. SHIOTSUKI and Y. TAKASHIMA, *J. Non-Cryst. Solids* **43** (1981) 115.
6. J. S. van WIERINGEN, *Phillips Tech. Rev.* **28** (1967) 33.
7. J. J. van LOEF and A. B. van GROENOU, Proceedings of International Conference on Magnetism, Nottingham, 1964, p. 646.
8. J. J. van LOEF and P. J. M. FRANSSEN, *Phys. Lett.* **7** (1963) 225.
9. E. KREBER, U. GONSER, A. TRAUTWEIN and F. E. HARRIS, *J. Phys. Chem. Solids* **36** (1975) 263.
10. H. KOJIMA, in "Ferromagnetic Materials", edited by E. D. Wohlfarth (North-Holland Publishing, New York, 1982) p. 305.
11. I. G. RENSEN and I. S. van WIERINGEN, *Solid State Commun.* **1** (1969) 1139.
12. J. BERETKA and M. J. RIDGE, *J. Chem. Soc.* **A3** (1968) 2463.
13. H. H. WICKMAN and C. F. WAGNER, *J. Chem. Phys.* **51** (1969) 435.
14. V. F. BELOV, T. A. KHIMICH, M. N. SHIPCO, I. S. ZHELVDEV, E. V. KORNEEV and N. S. OVANESYAN, *Sov. Phys. JETP* **37** (1974) 1089.
15. P. K. GALAGHEV, J. B. MACHESNEY and D. N. E. BUCHANAN, *J. Chem. Phys.* **41** (1964) 2429.
16. *Idem, ibid.* **45** (1966) 2466.
17. S. RAM, D. BAHADUR and D. CHAKRAVORTY, *J. Non-Cryst. Solids* **88** (1986) 311.

*Received 29 October 1991*
*and accepted 10 January 1992*